

We are IntechOpen, the world's leading publisher of Open Access books Built by scientists, for scientists

4,800

Open access books available

122,000

International authors and editors

135M

Downloads

Our authors are among the

154

Countries delivered to

TOP 1%

most cited scientists

12.2%

Contributors from top 500 universities



WEB OF SCIENCE™

Selection of our books indexed in the Book Citation Index
in Web of Science™ Core Collection (BKCI)

Interested in publishing with us?
Contact book.department@intechopen.com

Numbers displayed above are based on latest data collected.
For more information visit www.intechopen.com



In situ photochemically assisted synthesis of silver nanoparticles in polymer matrixes

Lavinia Balan, Jean-Pierre Malval and Daniel-Joseph Loughnot
*Institut de Science des Matériaux de Mulhouse LRC 7228,
 15 rue Jean Starcky, 68093 Mulhouse
 France*

1. Introduction

The synthesis of dispersed nanoparticles is essential for many advanced applications because of their novel properties that are greatly different from those of corresponding bulk substances. During the past years, a whole bunch of synthetic methods of metal nanoparticles (NPs) have been developed: chemical, photochemical and thermal. Amongst them, the photochemical method has attracted much attention due to it being a versatile and convenient process with distinguishing advantages such as space-selective fabrication (Sakamoto et al., 2009). This method was the key of the development of silver photography but recent advances in the chemistry of metal NPs and nanomaterials gave it a new lease of life. One of the main interests of metal NPs stems from their unique physical properties, which can be addressed by the chemical control of their shape and size (Burda et al., 2005).

For instance, silver nanoparticles with spherical shape and nanometer size exhibit a very intense absorption band in the visible region due to the surface plasmon resonance. The absorption coefficient can be orders of magnitude larger than strongly absorbing organic chromophores. Besides, the enhanced electromagnetic fields generated in the close-proximity of the metal surface have a strong influence on the local environment which is illustrated by surface-enhanced Raman scattering (SERS) or by metal-enhanced fluorescence process. Nanocomposite materials combine the different properties of the components. However, in a bulk medium, the benefit of these unique performances mainly relies on the homogeneous dispersion of uniformly shaped and sized particles into the matrix. Generally, metal-polymer nanocomposites are obtained via multi-step methods. Thus, silver nanoparticles can be produced beforehand, and then dispersed into a polymerizable formulation to obtain self-assembly functionalized structures. However, besides the specific hazards related to handling dry nanoparticles, this “*ex-situ*” method is limited by the difficulty to control their monodispersity over a large scale (Balan et al, 2006, 2008).

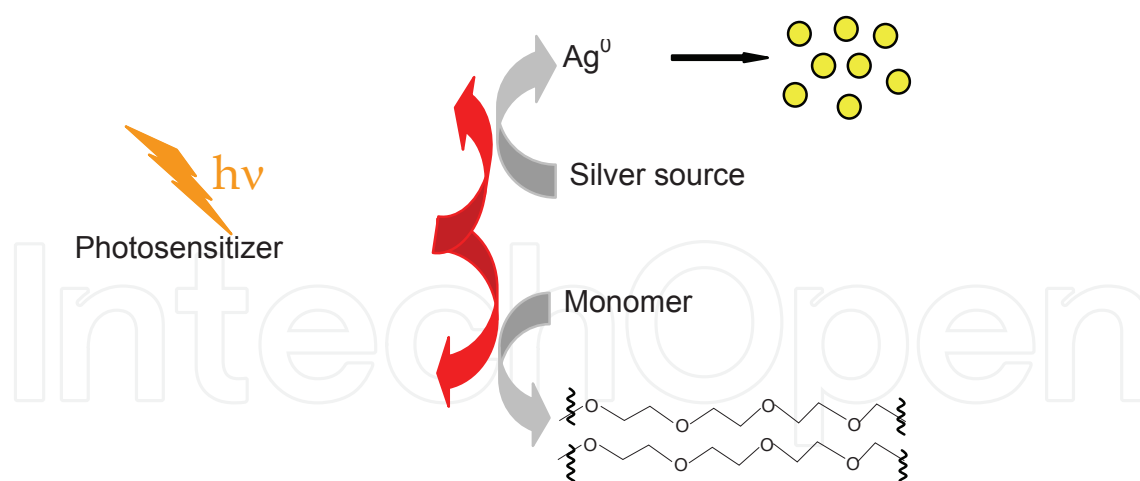
In the “*in-situ*” approach, the metal nanoparticles are generated in a polymerizable medium from cationic precursors that exhibit better dispersion ability and that undergo facile chemical or photochemical reduction.

This study focuses on the *in-situ* synthesis of silver nanoparticles in polymer matrix through photo-assisted processes. *In-situ* photochemical fabrication is one of the most powerful

approach to synthesize metal NPs/polymer nanocomposites. Furthermore, embedding nano-sized metal NPs into polymer matrix has attracted much interest because these materials open new perspectives; they combine properties from both inorganic and organic systems. Thus, metal NPs homogeneously dispersed in polymer matrixes are widely investigated. They are already used as sensors (Freeman et al., 1995; McConnell et al., 2000; Duan et al., 2001), as materials with solvent switchable electronic properties (Holmes et al. 2000), as optical limiters or filters (Jin et al., 2001; Biswas et al., 2004), as optical data storage (Ouyang et al., 2004, 2005), surface plasmon enhanced random lasing media (Hao et al., 2007), catalytic applications (Boyd et al., 2006), or for antimicrobial coatings (Sambhy et al., 2006; Anyaogu et al., 2008). Up to now, the fabrication of metal/polymer nanocomposites in poly(methyl methacrylate) (PMMA), poly(vinyl alcohol) (PVA), poly(vinyl acetate) (PVAc), poly(vinyl carbazole) (PVK), polyimide films and N-isopropylacrylamide (NIPAM), diallyldimethylammonium chloride (DADMAC) was reported (Weaver et al. 1996; Malone et al., 2002; Hirose et al., 2004; Sakamoto et al., 2006, 2007).

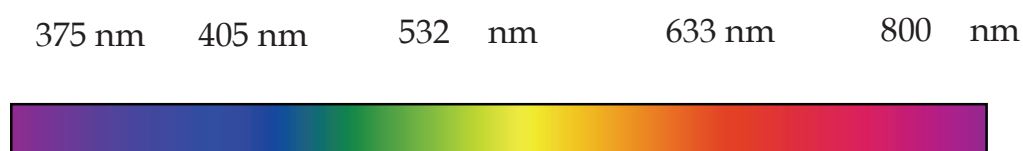
Similarly to what is widely-known in homogeneous solution, direct photoreduction and photosensitization are powerful approaches for the *in-situ* synthesis in polymer matrixes (Balan et al., 2008, 2009; Yagci et al., 2008). The heart of the photochemical approach is the generation of M^0 in such conditions that their precipitation is thwarted. M^0 can be formed through direct photoreduction of a silver source, silver salt or complex, or reduction of silver ions using photochemically generated intermediates, such as radicals.

The photoreduction is often promoted by dyes dispersed or dissolved in the polymer or present in the chemical structure of the matrix. In this one-step approach, we report a strategy involving the photoinduced formation of homogeneous silver nanoparticles in an acrylate polymer stemming from a crosslinking photopolymerization of an acrylate monomer (Scheme 1).



Scheme 1. Scheme of photochemical synthesis

Finally, no mean advantage of this *in situ* synthetic route to NPs and polymer/metal nanocomposite is its high flexibility in terms of actinic wavelengths used to trigger the photochemically assisted reduction of metal precursors (Scheme 2). Several formulations using laser sources with emissions ranging from the near-UV to the near-IR will exemplify this interesting feature.



Scheme 2. The laser lines used to generate silver NPs *in situ* in polymerizable formulations

2. General Techniques

The absorption spectra and kinetic follow-ups were recorded with a Perkin Elmer Lambda 2 spectrometer. A FluoroMax 4 Luminescence Spectrometer was used for the fluorescence and time-gated phosphorescence measurements. Low temperature experiments were carried out in a glassy matrix of isopropanol using a 5-mm diameter quartz tube inside a Dewar filled with liquid nitrogen. The emission spectra were spectrally corrected in all cases.

The reference photopolymerizable formulation contained Eosin Y (0.1 wt %), Methyl-diethanolamine - MDEA (3 % wt) and AgNO_3 (1 wt %) in acrylate monomer. It was sandwiched between two glass plates with a calibrated thickness wedge setting the optical path length to ca 30 μm . Photochemical reactions were carried out at 532 nm with a cw Verdi laser from Coherent. The progress of the reaction was monitored via UV-Vis absorption spectroscopy. The other formulations with various spectral sensitivity windows were formulated according to the same principle.

The photopolymerization was followed up *in situ* by real-time Fourier transformed infrared spectroscopy with an AVATAR 360 FTIR spectrometer from Nicolet. The laminated formulation (typ. 25 μm thick), deposited on a BaF_2 pellet, was irradiated at 532 nm with a green laser diode module from Crystallaser. The conversion rates were deduced from the disappearance of the vinyl C=C stretching vibration band at 1630 cm^{-1} .

Transmission electron microscopy (TEM) was used to characterize the size and shape of Ag nanoparticles. The nanocomposites were cut by means of a microtome (LKB model 8800) and placed onto the observation grid to get their TEM images. Transmission electron microscopy measurements were carried out at 200 kV using a Philips CM20 instrument with Lab6 cathode.

3. Results and discussion

The key step of the process is the reaction of silver cations with photogenerated transient species that are able to both reduce them to silver metal atoms and initiate the polymerization of the host medium. Two classes of photoinduced reactions were used to produce these primary radicals. The first one is based on the reaction of an electron rich molecule (amine, thiol, ether...) with the highly oxidant triplet state of a sensitizer excited upon absorption of the actinic photons. The second one involves the direct homolytic photocleavage of a sigma bond (mainly C-C bonds adjacent to a carbonyl).

3.1 Photo-oxidation – Activation at 532 nm

A dual system based on Eosin Y (E) and N-methyl diethanolamine (MDEA) was used to simultaneously photogenerate silver nanoparticles and photoinitiate the free radical polymerization. After a mechanistic analysis of the photoprocess by steady state spectroscopy, the elementary steps leading to the metal nanocomposite are correlated to structural properties of the reactants.

3.1.1 Mechanistic aspect of Ag nanoparticles photogeneration in solution

Figure 1 shows the lowest energy absorption band of EO^{2-} localized in the 450-575 nm region with a maximum at 530 nm in acetonitrile. The fluorescence spectrum of EO^{2-} is mirror image of its absorption band with a slight Stokes shift (535 cm^{-1}) suggesting a weak geometrical relaxation in the singlet state.

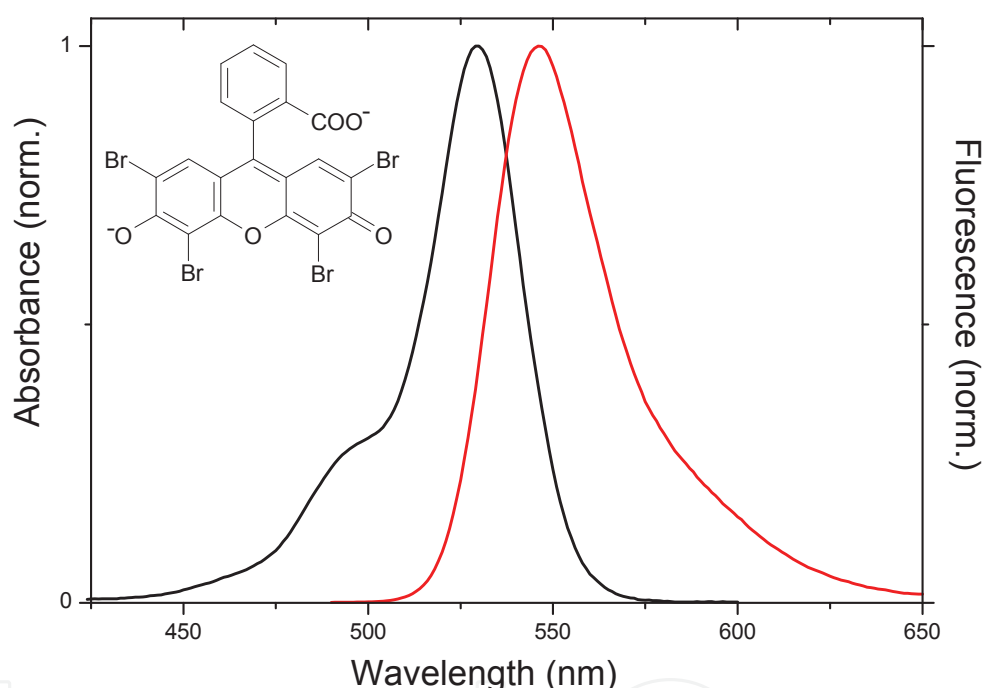


Fig. 1. Normalized absorption and fluorescence spectra of Eosin Y (solvent : acetonitrile)

Figure 2 shows the evolution of the absorption spectrum of EO^{2-} upon addition of increasing amounts of AgNO_3 in an alkaline solution of acetonitrile. The last absorption band is progressively shifted to the red ($\Delta\lambda_{\text{max}} = +4 \text{ nm}$) and the presence of two isosbestic points located at 498 nm and 530 nm indicates the presence of an equilibrium in the ground state. The presence of two isosbestic points located at 498 nm and 530 nm clearly indicates the occurrence of an equilibrium in the ground state. Moreover, the addition of tetra-N-butylammonium hexafluoroborate ($3 \times 10^{-2} \text{ M}$) excludes any variation of the ionic strength during the reaction. Therefore, these observations can be ascribed to a complexation reaction of Ag^+ by EO^{2-} which leads to the formation of an ion-pair complex $[\text{EO-Ag}]$. Under the same conditions, fluorescence emission shifts to the red ($\Delta\lambda_{\text{max}} = +5 \text{ nm}$) with a slight decrease in intensity while the fluorescence lifetime decreases from 4.05 ns to 3.80 ns.

Because the acidic character of the hydroxylic group is stronger than that of the carboxylic group (Levillain & Fompeydie, 1985; Moser & Grätzel, 1984), such a cation exchange reaction should mainly involve the chelation of silver cation by the 'phenolate' oxygen. This is also in line with the Pearson's hard-soft acid-base (HSAB) principle (Pearson, 1963, 1968) which presumes a better stabilizing interaction of Ag^+ (Soft Lewis acid) with the phenolate group than with the carboxylate function. However, the participation of the carboxylate function in the coordination reaction cannot be excluded. The inset of Figure 3 shows the best-fitting of the experimental data using the method of least squares; $\log K_{1:1}$ exhibits a high value of $\text{ca. } 4.7 \pm 0.3$ whereas $\log K_{1:2}$ has a value of $\text{ca. } 5.0 \pm 0.4$. Such a slight difference suggests that the formation of the [1:2] complex can be reasonably neglected under the experimental conditions of this work (i.e. $[\text{Ag}^+]/[\text{EO}^{2-}] < 50$).

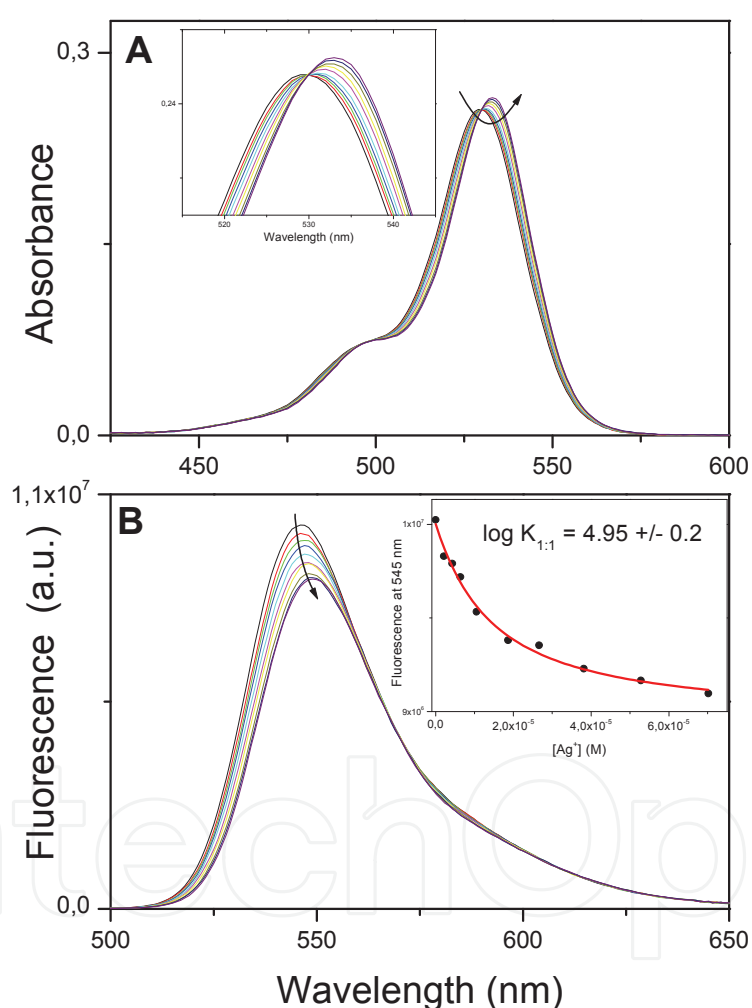


Fig. 2. (A) Evolution of the absorption spectrum of Eosin upon addition of AgNO_3 (solvent: acetonitrile), Inset: Isosbestic point at 530 nm. (B) Evolution of the fluorescence spectrum of Eosin upon addition of AgNO_3 (solvent acetonitrile), Inset: Dependence of fluorescence intensity at 545 nm vs. concentration of silver cations (circles). Best fitting curve (red line)

Results of the steady state photolysis experiments are shown on figure 3. The changes in the spectral features observed upon laser excitation of Eosin Y and AgNO_3 (50 eq.) solution in

acetonitrile are reported on Figure 3. Upon increasing the exposure, the absorption band of EO^{2-} was progressively fading away while no trace of the formation of silver nanoparticles could be detected. The same photolysis experiment was then performed in an acetonitrile solution containing Eosin Y, AgNO_3 and MDEA. In this case, a new band centred around 435 nm and characteristic of the surface plasmon (SP) of silver nanoparticles was clearly developing (Figure 3). The only species capable of reducing Ag^+ in the presence of MDEA and under visible irradiation is a transient photoproduct deriving from Eosin. This suggests that the formation of silver nanoparticles was promoted by the excited state of EO^{2-} and confirms the mediating role of MDEA. Thus, the sequence of reaction would involve first, an electron transfer from the amine to $^3\text{EO}^{2-}$, and then a proton transfer within the ion pair formed between amine radical cation and Eosin radical anion (Jones & Chatterjee, 1988; Kepka & Grossweiner, 1971; Rele et al., 2004; Janata et al., 1994; Burget et al., 1999). Hence, the reaction should initially produce an α -aminoalkyl radical and the conjugated acid of semi-reduced Eosin ($\text{EOH}^{\bullet 2-}$). The photogenerated α -aminoalkyl that is known as a strongly reductive species can convert efficiently Ag^+ to Ag^0 as follows:

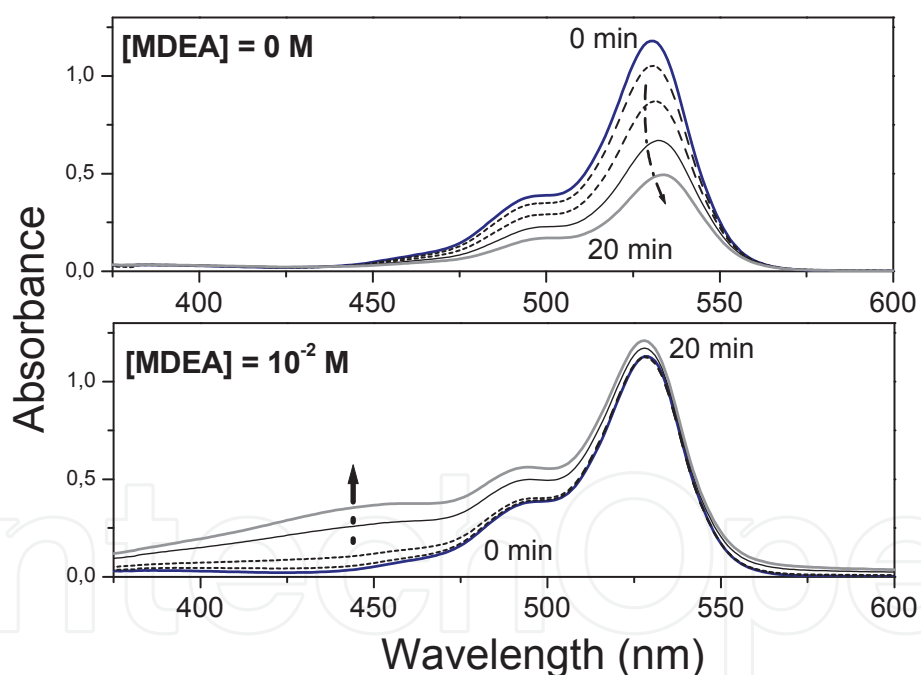
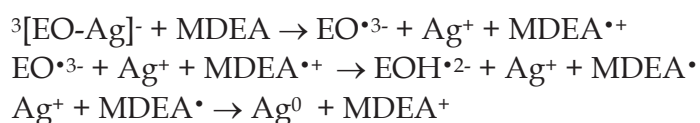


Fig. 3. Evolution of the absorption spectra of two irradiated mixtures in acetonitrile ($\lambda_{\text{irr}} = 532 \text{ nm}$) (a) without MDEA and (b) with MDEA

3.1.2 In situ generation of Ag^0 embedded in a crosslinked polymer.

An acrylate formulation which contained EO^{2-} (0.1 wt %) and MDEA (3 % wt) (Espanet et al., 1999; Rathore et al., 2005). was mixed with AgNO_3 (1 wt %) and then photopolymerized at 532 nm (2.5 mW.cm^{-2}). The conversion of the acrylate double bonds was followed up by real-time FTIR at 1630 cm^{-1} and was compared with the conversion rate of a reference formulation without AgNO_3 (Figure 4).

Basically, addition of Ag^+ does not perturb the polymerization kinetics. After a 10-min exposure, the reference sample turned from pink to colourless whereas the sample with Ag^+ turned from pink to brown-yellowish. The visible absorption band of EO^{2-} decreased progressively whereas the plasmon band developed in the 350-500 nm region with a maximum at 437 nm and a FWHM of 115 nm. MDEA acts both as an electron donor in the photoinitiation process (Fouassier & Chesneau, 1991) and as a basic agent that quantitatively converts Eosin into dianionic form. Figure 5 shows the photobleaching of Eosin Y which goes concomitantly with the growth of the surface plasmon band. The existence of an isosbestic point at 480 nm strongly suggests a simple reaction between EO^* and Ag^+ leading to reduced EO^{2-} and Ag^0 . This assumption was corroborated by the linear correlation obtained when plotting the absorbance at 532 nm *vs.* absorbance at 432 nm (inset Figure 5). This latter species is then involved into the photo-initiating process in the presence of MDEA.

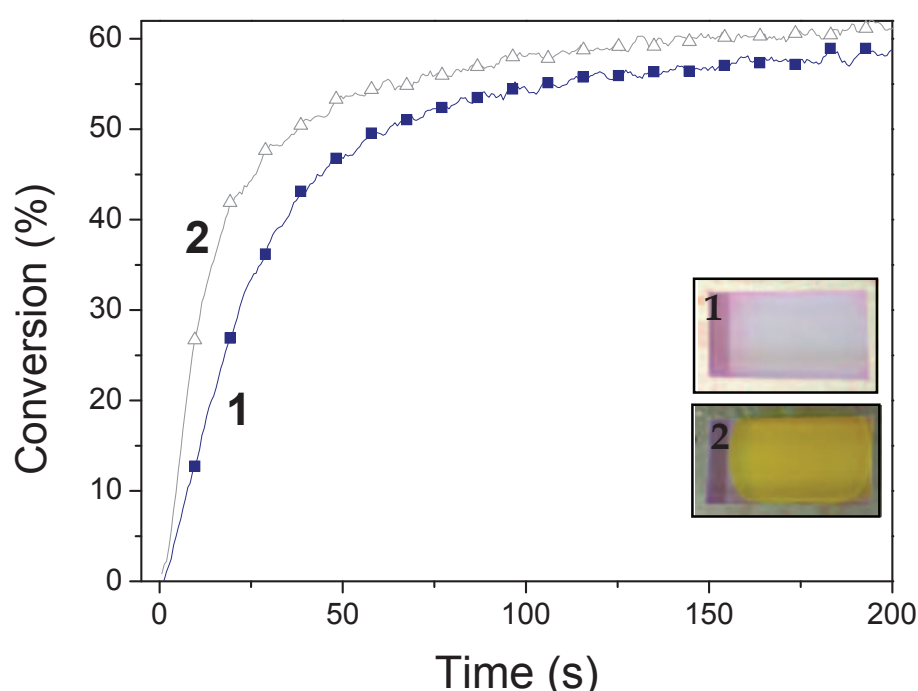


Fig. 4. Real-time FTIR kinetics conversion curves of the acrylate double bonds for visible curing at 532 nm: (1) EO^{2-} / MDEA, 0.1 wt % / 3 wt % and (2) EO^{2-} / MDEA / AgNO_3 , 0.1 wt % / 3 wt % / 1 wt %. Inset: View of 30 μm thick samples (1) and (2) after curing.

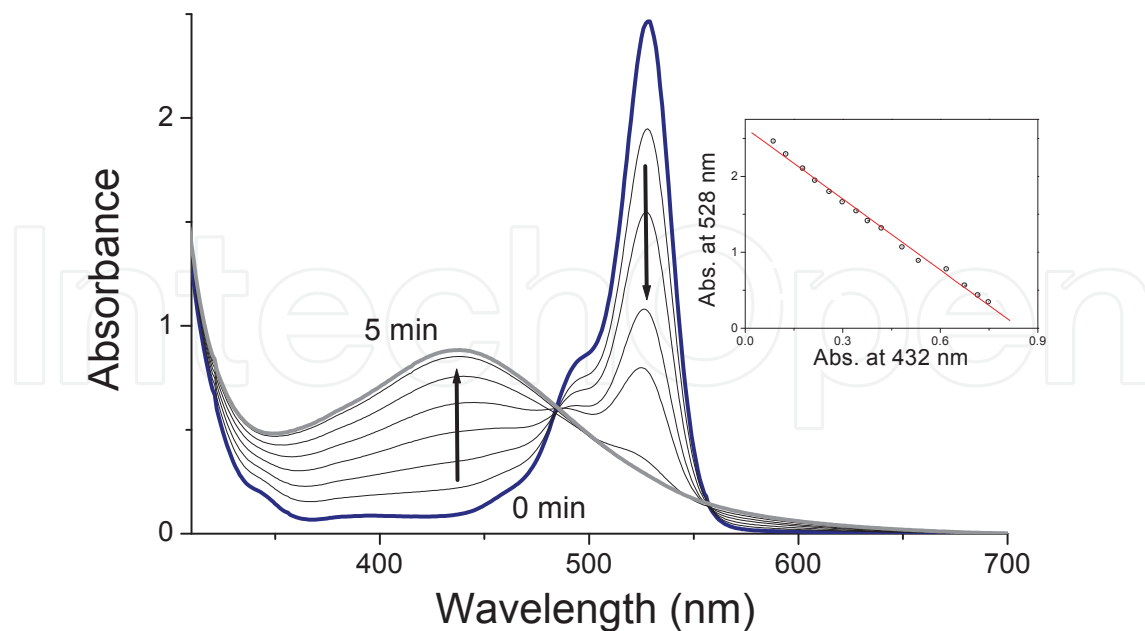


Fig. 5. Absorption evolution of the Eosin and silver NPs during photopolymerization, EO (0.1 wt %) / MDEA (3 wt %) / AgNO_3 (1 wt %). Inset: Linear correlation between absorptions at 532 nm and 432 nm.

Transmission electron microscopy analysis of the sample indicated the formation of monodisperse spherical particles whose diameters are in the 3 to 7 nanometer range. Analysis of a population of ca. hundred silver nanoparticles from a portion of the grid indicated that their average diameter was 5.0 ± 0.7 nm (Figure 6). The particles were homogeneous in size and no agglomeration was observed.

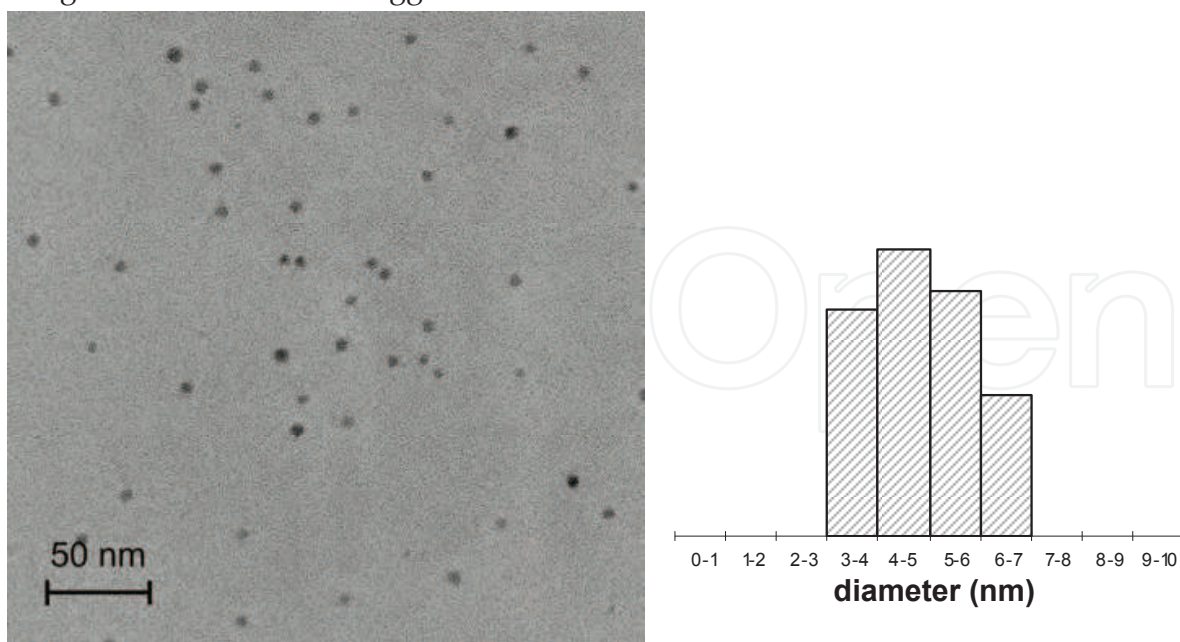
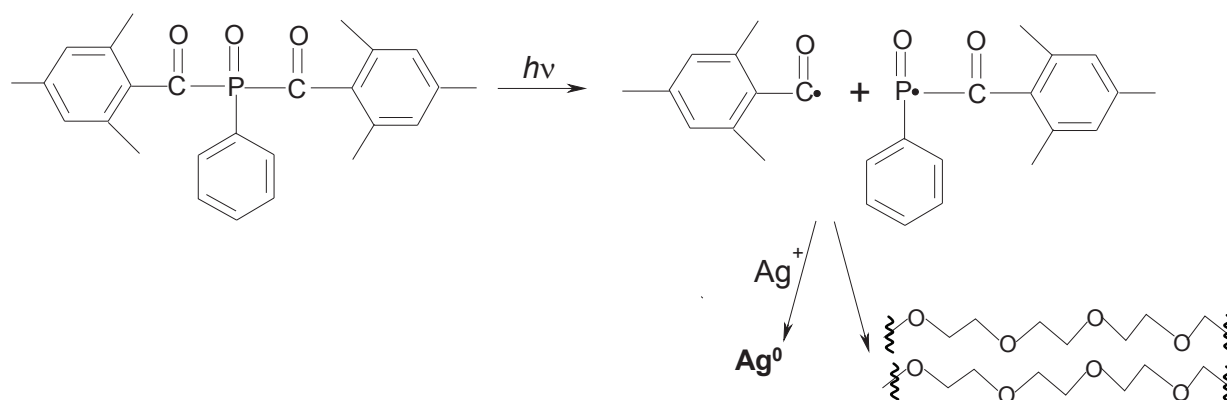


Fig. 6. TEM image of silver nanoparticles embedded in a polyacrylate matrix and histogram of the diameter distribution obtained from this TEM image

3.2 Photocleavage – Activation at 405 nm

An acylphosphine oxide was used as free radical source upon irradiation with near-UV light. Usually, this photoinitiator serves to initiate the photopolymerization of top-coatings formulations by UV A and deep blue sources. In its triplet state, bis-(2,4,6-trimethylbenzoyl)-phenylphosphine oxide (Irgacure 819) is known to undergo α -cleavage and generate a pair of radicals as shown on scheme 3. Indeed, the homolytic photocleavage of the C-P bond generates 2,4,6-trimethylbenzoyl and phenylphosphonyl radicals. In the present application, this photoinitiator simultaneously induces the formation of silver nanoparticles through reduction of AgNO_3 and initiates the radical polymerization of the acrylic resin. Thus, irradiation of Irgacure 819 in polyethylene glycol diacrylate monomer (SR 344, Mw = 508 g/mol) in the presence of AgNO_3 led to its reduction with rapid generation of both metallic silver and radical initiation of the crosslinking polymerization without any spurious side reactions. The formation of silver particles during the polymerization was confirmed by UV-Vis absorption (the color of the sample turned to brown-yellow).



Scheme 3. Photocleavage mechanism of Irgacure 819.

Figure 7 shows the typical evolution of the UV-Visible spectrum of the Irgacure 819/ Ag^+ solution upon increasing the incident dose of actinic light. Before irradiation, Irgacure 819 exhibited a peak at about 375 nm and a strong absorption at 405 nm. As the photolysis proceeded, the absorption of Irgacure 819 decreased; the photo-generated radicals reduced Ag^+ to Ag^0 while a new band grew up at around 410 nm that corresponds to the surface plasmon resonance of silver metal particles. It must be emphasized that no metal NPs are generated when AgNO_3 was irradiated under the same photonic conditions in isopropanol in the absence of Irgacure 819. This observation thus, excluded the intervention of any photo-thermal effect in the process generating NPs.

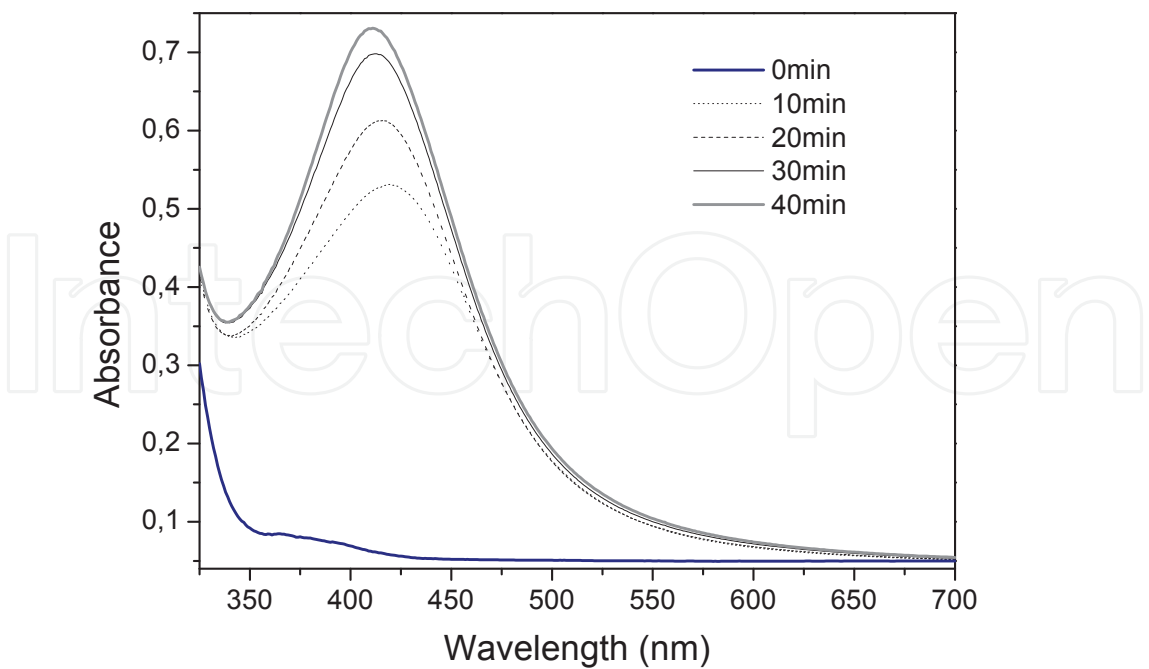


Fig. 7. Evolution of Irgacure 819 and silver absorptions during exposure of a photosensitive silver salt

The bright-field TEM micrograph (Figure 8) of the UV-cured films confirmed the synthesis of spherical particles and showed the well dispersed silver nanoparticles without macroscopic aggregation. The average diameter of the silver nanoparticles was 4.3 ± 0.4 nm.

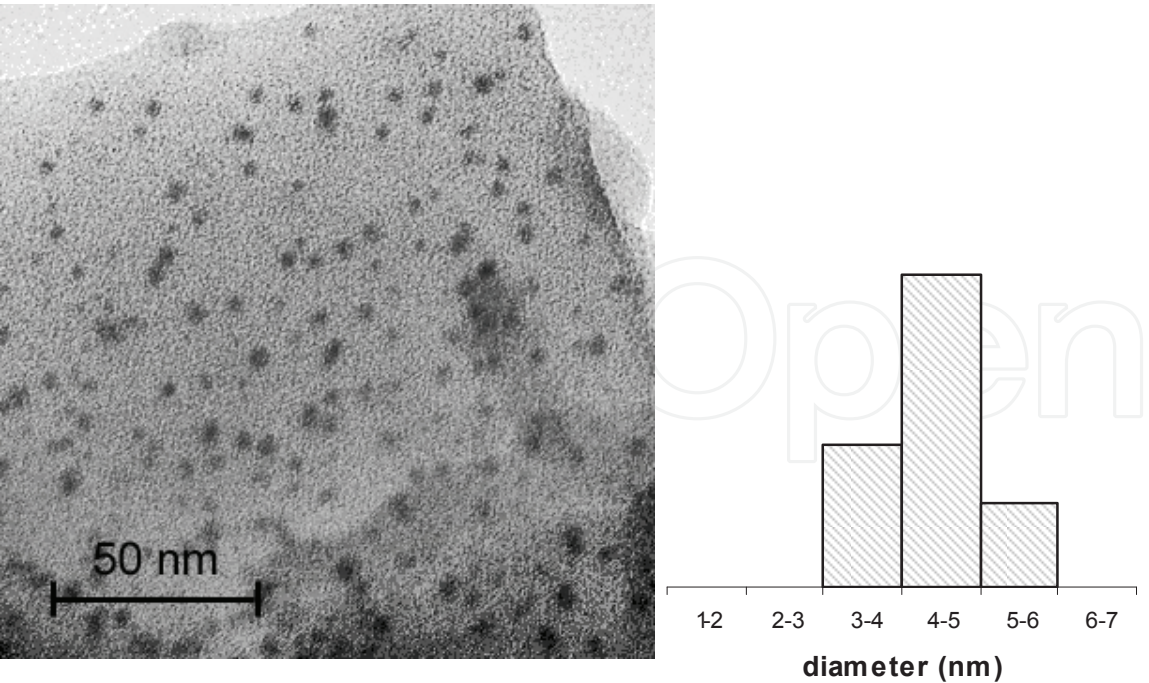


Fig. 8. TEM images of silver nanoparticles embedded in polymer matrix with the respective size distribution.

4. Conclusion

The photo-induced synthesis of silver nanoparticles was carried out in a wide range of experimental conditions: variety of actinic wavelengths (table 1), variety of photoreduction media (solution and acrylic monomer).

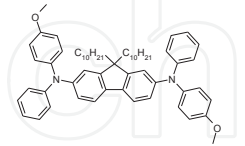
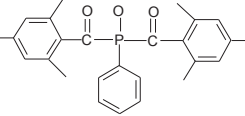
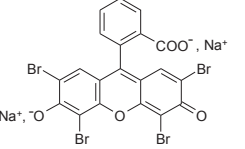
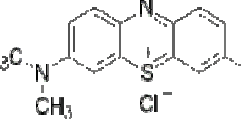
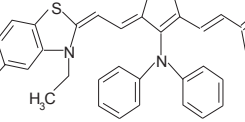
Molecule name	Structure	Wavelength (nm)	Co-initiator
2,7-diaminofluorene derivative		375 nm	*
Bis (2,4,6-trimethylbenzoyl) phenylphosphine oxide		405 nm	-
Eosin Y		532 nm	*
Methylene blue		633 nm	*
Cyanine dye		800 nm	*

Table 1. Names and chemical structures of the photoinitiators used

When the dye and silver cations are mixed together in the monomer resin, both photoreduction and photoinitiation occur in parallel without interaction. Silver nanoparticles are homogenously distributed within the polymer network without macroscopic agglomeration and they do not affect the photopolymerization process. Polymer/metal nanocomposite materials are thus, produced within seconds from a liquid formulation.

The one-pot and one-step photochemical process turns out to be a verily innovative route to synthesize silver nanoparticles especially in polymer matrixes that, to top it all, affords high spatial resolution and temporal controllability.

A few reports mentioning the photoinduced synthesis of other geometries than spheres (tetraedrons, sticks...) appeared recently in the literature. However, obtaining particles with well-defined geometries and narrow dispersity remains a challenging issue.

5. References

- Anyagou, K. C.; Fedorov, A. V. & Neckers, D. C. (2008). Synthesis, Characterization, and Antifouling Potential of Functionalized Copper Nanoparticles. *Langmuir*, 24, 4340-4346
- Balan, L. & Burget. D. (2006). Synthesis of metal /polymer nanocomposite by UV-radiation curing. *European Polymer Journal*, 42, 3180-3189
- Balan, L.; Schneider, R. & Lougnot, D. J. (2008). A new and convenient route to polyacrylate/silver nanocomposites by light-induced cross-linking polymerization. *Progress in Organic Coatings*, 62, 351-357
- Balan, L.; Jin, M.; Malval, J-P.; Chaumeil, H.; Defoin, A. & Vidal, L. (2008). Fabrication of silver nanoparticle-embedded polymer promoted by combined photochemical properties of 2,7-diaminofluorene derivative dye. *Macromolecules*, 41, 9359-9365
- Balan, L.; Malval, J-P.; Schneider, R.; Le Nouen, D. & Lougnot, D. J. (2009). In situ fabrication of polyacrylate-silver nanocomposite through photoinduced tandem reactions involving eosin dye. *Polymer*, DOI: 10.1016/j.polymer.2009.05.003.
- Boyd, D. A.; Greengard, L.; Brongersma, M.; El-Naggar, M. Y. & Goodwin, D. G. (2006). Plasmon-assisted chemical vapor deposition. *Nanolett.*, 6, 2592-2597
- Burda, C.; Chen, X. B.; Narayanan, R. & El-Sayed, M. A. (2005). Chemistry and properties of nanocrystals of different shapes. *Chem. Rev.*, 105(4), 1025-1102
- Burget, D.; Fouassier, J. P.; Amat-Guerri, F.; Mallavia, R. & Sastre, R. (1999). Enhanced activity as polymerization photoinitiators of Rose Bengal and Eosin esters with an O-benzoyl- α -oxooxime group : The role of the excited state reactivity. *Acta Polym.*, 50, 337-346
- Duan, X.; Huang, Y.; Cui, Y.; Wang, J. & Lieer, C. M. (2001). In situ fabrication of silver nanoparticles in a photopolymer matrix. *Nature*, 409, 66-69
- Espanet, A.; Ecoffet, C. & Lougnot, D. J. (1999). PEW: Photopolymerization by evanescent waves . II - Revealing dramatic inhibiting effects of oxygen at submicrometer scale. *J Polym Sci A: Polym Chem.*, 37, 2075-2085.
- Fouassier, J-P. & Chesneau, E. (1991). Polymérisation induite sous irradiation laser visible, Le système éosine/photoamorceur ultra violet/amine. *Makromol. Chem.*, 192, 245-260
- Freeman, R. G.; Grabar, K. C.; Allison, K. J.; Bright, R. M.; Davis, J. A.; Guthrie, A. P.; Hommer, M. B.; Jackson, M. A.; Smith, P. C.; Walter, D. G. & Natan, M. J. (1995) Self-assembled metal colloid monolayers: An approach to SERS substrates. *Science*, 267, 1629
- Hao, F.; Nehl, C. L.; Hafner, J. H. & Nordlander, P. (2007). Plasmon resonances of a gold nanostar. *NanoLett.*, 7(3), 729-732
- Hirose, T.; Omatsu, T.; Sugiyama, M.; Inasawa, S. & Koda, S. (2004). Au-nano-particles production by pico-second ultra-violet laser deposition in Au-ion doped PMMA film. *Chem. Phys. Lett.*, 390, 166-169
- Holmes, J. D.; Johnston, K. P.; Doty, R. C. & Korgel, B. A. (2000). Control of thickness and orientation of solution-grown silicon nanowires. *Science*, 287, 1471-1473
- Janata, E.; Henglein, A. & Ershovt, B. G. (1994). First clusters of Ag⁺ ion reduction in aqueous solution. *J. Phys. Chem.*, 98, 10888-10890

- Jones, G. & Chatterjee, S. (1988). Steric control of distance parameters and the yield of charge- carriers in photochemical electron-transfer the quenching of eosin-Y by hindered phenols. *J. Phys. Chem.*, 92, 6862-6864
- Kepka, A. G. & Grossweiner, L. I. (1971). Photodynamic oxidation of iodide ion and aromatic amino acids by eosin. *Photochem. Photobiol.*, 14, 621-639
- Levillain, P. & Fompeydie, D. (1985). Determination of equilibrium constants by derivative spectrophotometry. Application to the pK_as of Eosin. *Anal. Chem.*, 57, 2561-2563
- Malone, K, Weaver, S.; Taylor, D.; Cheng, H.; Sarathy, K. P. & Mills, G. (2002). Formation Kinetics of Small Gold Crystallites in Photoresponsive Polymer Gels. *J. Phys. Chem. B*, 106, 7422-7431
- McConnell, W. P.; Novak, J. P.; Brousseau, L. C.; Fuierer, R. R.; Tenent, R.C. & Feldheim, D. L. (2000). Electronic and Optical Properties of Chemically Modified Metal Nanoparticles and Molecularly Bridged Nanoparticle Arrays. *J. Phys. Chem. B*, 104, 8925-8930
- Moser, J.; & Grätzel, M. (1984). Photosensitized electron injection in colloidal semiconductors. *J. Am. Chem. Soc.*, 106, 6557-6564
- Ouyang, J.; Chu, C.-W.; Szmanda, C. R.; Ma, L. & Yang, Y. (2004). Programmable polymer thin film and non-volatile memory device. *Nat. Mat.*, 3, 918-922
- Ouyang, J.; Chu, C.-W.; Sieves, D.; Yang, Y. (2005). Electric-field-induced charge transfer between gold nanoparticle and capping 2-naphthalenethiol and organic memory cells. *Appl. Phys. Lett.*, 86, 123507-123513
- Pearson, R. G. (1963). Hard and Soft Acids and Bases. *J. Am. Chem. Soc.*, 85, 3533-3539
- Pearson, R. G. (1968). Hard and soft acids and bases. HSAB, Part I, Fundamental principles. *J. Chem. Educ.*, 45, 581-587
- Rathore, R.; Chebny, V. J. & Abdelwahed, S. H. (2005). A versatile and conformationally adaptable fluorene-based receptor for efficient binding of silver cation. *J. Am. Chem. Soc.*, 127, 8012-8013
- Rele, M.; Kapoor, S.; Sharma, G. & Mukherjee, T. (2004). Reduction and aggregation of silver and thallium ions in viscous media. *Phys. Chem. Chem. Phys.*, 6, 590-595
- Sakamoto, M.; Tachikawa, T.; Fujitsuka, M. & Majima, T. (2000). Acceleration of Laser-Induced Formation of Gold Nanoparticles in a Poly(vinyl alcohol) Film. *Langmuir*, 22, 6361-6366
- Sakamoto, M.; Tachikawa, T.; Fujitsuka, M. & Majima, T. (2007). Photochemical Formation of Au/Cu Bimetallic Nanoparticles with Different Shapes and Sizes in a PVA Film. *Adv. Funct. Mater.*, 17, 857-862
- Sakamoto, M.; Fujitsuka, M. & Majima, T. (2009). Light as a construction tool of metal nanoparticles: Synthesis and mechanism. *J. Photochem and Photobiol C: Photochem Reviews* 10(1) 33-56
- Sambhy, V.; MacBride, M. M.; Peterson, B. R. & Sen, A. Silver Bromide Nanoparticle Polymer Composites: Dual Action Tunable Antimicrobial Materials. *J. Am. Chem. Soc.*, (2006). 128, 9798-9808
- Shipway, A N.; Katz, E.; Willner, I.; (2000). Nanoparticle Arrays on Surfaces for Electronic, Optical, and Sensor Applications. *Chem Phys Chem*, 1, 18-52
- Weaver, S.; Taylor, D.; Gale, W. & Mills, G. (1996). Photoinitiated Reversible Formation of Small Gold Crystallites in Polymer Gels. *Langmuir*, 12, 4618-4620

IntechOpen

IntechOpen



Silver Nanoparticles

Edited by David Pozo Perez

ISBN 978-953-307-028-5

Hard cover, 334 pages

Publisher InTech

Published online 01, March, 2010

Published in print edition March, 2010

Nanotechnology will be soon required in most engineering and science curricula. It cannot be questioned that cutting-edge applications based on nanoscience are having a considerable impact in nearly all fields of research, from basic to more problem-solving scientific enterprises. In this sense, books like “Silver Nanoparticles” aim at filling the gaps for comprehensive information to help both newcomers and experts, in a particular fast-growing area of research. Besides, one of the key features of this book is that it could serve both academia and industry. “Silver nanoparticles” is a collection of eighteen chapters written by experts in their respective fields. These reviews are representative of the current research areas within silver nanoparticle nanoscience and nanotechnology.

How to reference

In order to correctly reference this scholarly work, feel free to copy and paste the following:

Lavinia Balan, Jean-Pierre Malval and Daniel-Joseph Lougnot (2010). In Situ Photochemically assisted Synthesis of Silver Nanoparticles in Polymer Matrixes, Silver Nanoparticles, David Pozo Perez (Ed.), ISBN: 978-953-307-028-5, InTech, Available from: <http://www.intechopen.com/books/silver-nanoparticles/in-situ-photochemically-assisted-synthesis-of-silver-nanoparticles-in-polymer-matrixes>

INTECH
open science | open minds

InTech Europe

University Campus STeP Ri
Slavka Krautzeka 83/A
51000 Rijeka, Croatia
Phone: +385 (51) 770 447
Fax: +385 (51) 686 166
www.intechopen.com

InTech China

Unit 405, Office Block, Hotel Equatorial Shanghai
No.65, Yan An Road (West), Shanghai, 200040, China
中国上海市延安西路65号上海国际贵都大饭店办公楼405单元
Phone: +86-21-62489820
Fax: +86-21-62489821

© 2010 The Author(s). Licensee IntechOpen. This chapter is distributed under the terms of the [Creative Commons Attribution-NonCommercial-ShareAlike-3.0 License](https://creativecommons.org/licenses/by-nc-sa/3.0/), which permits use, distribution and reproduction for non-commercial purposes, provided the original is properly cited and derivative works building on this content are distributed under the same license.

IntechOpen

IntechOpen